Biochemical Pharmacology 243 (2026) 117497

Contents lists available at ScienceDirect

Biochemical Pharmacology

journal homepage: www.elsevier.com/locate/biochempharm

Ribosomal protein L5 (RPL5/uL18) I60V mutation is associated to increased translation and modulates drug sensitivity in T-cell acute lymphoblastic leukemia cells

Lorenza Bacci [a,1], Daniela Pollutri [a,b,1], Israt Jahan Ripa [a,1], Michael D'Andrea [a], Virginie Marchand [d], Yuri Motorin [d,e], Anne-Marie Hesse [c], Yohann Couté [c], Kamil Filipek [a], Marianna Penzo [a,b,*]

[a] Department of Medical and Surgical Sciences (DIMEC) and Center for Applied Biomedical Research (CRBA), Alma Mater Studiorum University of Bologna, Via Massarenti 9, 40138 Bologna, Italy
[b] IRCCS Azienda Ospedaliero-Universitaria di Bologna 40138 Bologna, Italy
[c] Univ. Grenoble Alpes, INSERM, CEA, UA13 BGE, CNRS, UAR2048, F-38000 Grenoble, France
[d] UAR2008 IBSLor CNRS-INSERM, Université de Lorraine, BioPole, F54000 Nancy, France
[e] UMR7365 IMoPA, CNRS, Université de Lorraine, BioPole, F54000 Nancy, France

ARTICLE INFO

Keywords:
Cancer
Ribosomes
Target therapy
Translation
Translation inhibitors
CRISPR-Cas

ABSTRACT

Somatic mutations in ribosomal proteins (RPs), including RPL5, have been reported in approximately 10 % of pediatric patients with T-cell acute lymphoblastic leukemia (T-ALL). In cancer, the incorporation of mutant RPs into ribosomes often disrupts canonical ribosome function, thereby contributing to disease development. In this study, we aimed to characterize the effects of the RPL5-I60V mutation in the context of T-ALL, focusing on its impact on translation and cellular responses to a panel of compounds in vitro. Using CRISPR-Cas9, we generated a homozygous knock-in mutant in Jurkat cells and investigated its effects on ribosome biogenesis. We observed both quantitative and qualitative alterations in the production of the large ribosomal subunit. Ribosomes containing the mutant RPL5 protein exhibited intrinsically increased protein synthesis activity, which correlated with enhanced cellular proliferation. We then evaluated the response of these mutant cells to a panel of compounds targeting protein synthesis at various levels—including an MNK1 inhibitor, metformin, silvestrol, homoharringtonine, anisomycin, resveratrol, and hygromycin B—as well as cytarabine, a chemotherapeutic agent commonly used in T-ALL treatment. Our results showed that the RPL5-I60V mutation confers increased sensitivity to most of these compounds, with the exception of hygromycin B.

This study advances our understanding of how oncoribosomes contribute to cancer pathogenesis and highlights the therapeutic potential of directly or indirectly targeting altered ribosomes, offering insights for the development of personalized treatment strategies.

Abbreviations: ABCB10, ATP binding cassette subfamily B member 10; ANI, Anisomycin; ARA-C, Cytarabine; ARL4C, ADP-ribosylation factor-like protein 4C; B3GNT2, UDP-GlcNAc:betaGal beta-1,3-N-acetylglucosaminyltransferase 2; CHX, Cycloheximide; ddPCR, digital droplet PCR; eIF4A, eukaryotic initiation factor-4A; eIF4E, eukaryotic translation initiation factor 4E; ERCC4, ERCC Excision Repair 4, Endonuclease Catalytic Subunit; ETFDH, electron transfer flavoprotein dehydrogenase; HHT, Homoharringtonine; HYG B, Hygromycin B; IRES, Internal Ribosome Entry Site; LRPPRC, Leucine Rich Pentatricopeptide Repeat Containing; MNK1, mitogen-activated protein kinase-interacting kinase 1; MTF, Metformin; mTOR, mechanistic target of rapamycin kinase; NOTCH1, notch receptor 1; NPC1, NPC intracellular cholesterol transporter 1; PHF6, PHD finger protein 6; PTI-1, Prostate Tumor Inducing gene-1; RNP, ribonucleoprotein; RP, Ribosomal Protein; RPL10, Ribosomal Protein *L*10; RPL11, Ribosomal Protein *L*11; RPL22, Ribosomal Protein L22; RPL5, Ribosomal Protein L5; RV, Resveratrol; ssODN, single-stranded-oligodeoxynucleotide; SIL, Silvestrol; T-ALL, T-cell acute lymphoblastic leukemia; TRIM27, tripartite motif containing 27; UPR, unfolded protein response.

* Corresponding author at: Department of Medical and Surgical Sciences (DIMEC) and Center for Applied Biomedical Research (CRBA), Alma Mater Studiorum University of Bologna, Via Massarenti 9, 40138 Bologna, Italy.
E-mail address: marianna.penzo@unibo.it (M. Penzo).

[1] Equal contribution.

https://doi.org/10.1016/j.bcp.2025.117497
Received 28 July 2025; Received in revised form 24 September 2025; Accepted 24 October 2025
Available online 31 October 2025

1. Introduction

T-cell acute lymphoblastic leukemia (T-ALL), accounting for ~15 % of pediatric ALL cases, is a highly aggressive hematologic malignancy marked by clonal expansion of immature T-lineage hematopoietic precursors infiltrating the bone marrow and expressing aberrant T-cell markers [1]. T-ALL is a molecularly heterogeneous disease, with onset and progression linked to the accumulation of genetic alterations in oncogenes and tumor suppressors involved in essential cellular functions [1]. Frequently mutated genes include T cell-specific transcription factors such as NOTCH1 (mutated in >60 % of cases) [1], as well as genes encoding epigenetic regulators (e.g., PHF6), tyrosine kinases, and signaling proteins (e.g., JAK/STAT pathway components) [2]. Recently, somatic mutations in ribosomal protein (RP) genes have been identified as novel drivers in pediatric T-ALL pathogenesis [3,4]. Somatic mutations in RPL5, RPL10 [4], RPL11 [5] and RPL22 [6] have been described with a cumulative frequency close to 10 % in pediatric T-ALL patients. RPs, along with rRNAs, form the ribosome's structural core, and their dysregulation or mutation is linked to various hematologic and solid tumors [7,8]. Heterozygous large deletions or point mutations in RPL5 were identified in several sporadic human tumors, including breast cancer, glioblastoma multiforme and melanoma [9–11]. In addition to being a component of the ribosome large subunit (60S), with important structural and functional activities [12], RPL5 has also multiple ribosome-independent functions, among which the regulation of ribosomal stress responses [13], of DNA repair mechanisms [14] and of transcription [15]. Consequently, genetic alterations in RPL5 can perturb multiple cellular processes, ultimately conferring distinct oncogenic properties to cancer cells. A principal outcome of RP mutations is the disruption of canonical ribosome function, resulting in the emergence of so-called "oncoribosomes" [7]. These aberrant ribosomes are proposed to exhibit functional specialization, potentially enabling the preferential translation of specific mRNA subsets in a context-dependent manner, thus contributing to the tumorigenic process [16,17]. This translational reprogramming represents an additional layer of gene expression regulation contributing to tumorigenesis [18].

Although, in the context of childhood T-ALL, currently available therapies, such as chemotherapy, lead to long-term remission for over 90 % of patients [19], relapse remains a relevant scenario. The main cause of relapse is the emergence of resistance mutations in leukemia cells [20]. Since most of the tumors are characterized by hyperproliferation and an increase in the rate of protein synthesis to sustain cellular growth, a growing list of compounds targeting different steps of translation and/or ribosome biogenesis has been tested, and in some cases approved, for the clinical treatment of different tumor types [21,22].

The development of drugs specifically targeting *oncoribosomes* would represent a promising therapeutic strategy in the perspective of personalized medicine [23]. In this study, we investigated the impact of mutated RPL5 on cellular phenotype and on the response to different therapeutic compounds, using a T-ALL cellular model in which we knocked in a prototypic RPL5 mutation (I60V). Our findings demonstrate that a single RPL5 mutation induces distinct phenotypic traits in cells, accompanied by changes in drug sensitivity that are strongly influenced by the compound's mechanism of action.

2. Materials and methods

2.1. Cellular model setup

Jurkat cells carrying the RPL5 c.178A > G (p.I60V) mutation were generated by CRISPR/Cas9 genome editing using the Alt-R™ CRISPR-Cas9 System (Integrated DNA Technologies, Coralville, IA, USA). Briefly, ribonucleoprotein (RNP) complexes were generated by combining 160 pmol of equimolar crRNA (custom, Table 1):tracrRNA duplex with 80 pmol of Cas9 endonuclease. RNP complexes and 5 μg of single strand HDR donor template (ssODN, Table 1) were mixed with 10^6 cells to a final volume of 100 μl in EP buffer (Optimem medium, ThermoFisher, Waltham, MA, USA) and electroporated by using Nepa21 electroporator system (Nepa Gene Co., Ltd, Chiba, Japan) using the following settings for poring: pulse 175 V, 5 ms length, 50 ms interval, and manufacturer's recommended protocol for transfer pulse. 48 h after electroporation, cells were checked for mutation knock-in efficiency by genotyping assay using a droplet digital PCR (ddPCR) approach (QX200 Bio-Rad Droplet Digital PCR System, Bio-Rad, San Francisco, CA, USA) with probes distinguishing the WT from the I60V allele (TaqMan® SNP Genotyping Assays, ThermoFisher, Waltham, MA, USA). Homozygous I60V-RPL5 growing clones were isolated by single cell cloning and ddPCR genotyping screening. Clones that tested negative for RPL5 mutations in the ddPCR screening were considered wild-type. RPL5 mutational status of selected clones was confirmed by Sanger sequencing (for primers sequences see Table 1). To bypass the potential impact of off-target alterations, all experiments were performed with two clones for both genotypes.

2.2. Cell culture and growth curve

Jurkat clones were maintained in RPMI medium supplemented with 20 % fetal bovine serum (FBS), 100 I.U./ml penicillin, 100 μg/ml streptomycin, and 2 mM L-glutamine. To overcome the biological variability intrinsic to clone-based experimental approaches, all experiments were carried out in parallel on 2 wt and 2 RPL5-I60V mutant clones.

For proliferation assay, a concentration of $1x10^6$ cells/ml was used for seeding the cells. Cell counting, performed in duplicate, was carried out every 24 h by Countess 3 device (Invitrogen, Carlsbad, California USA).

Table 1
Custom synthesized sequences.

crRNA	AAACAGAGATAUCAUUUGUCAGG	Integrated DNA Technologies (Coralville, IA, USA) AGG: PAM sequence
ssODN	5′-ACCCAAATACAGGATGATAGTTCGTGTGACAAACAGAGATGTCATTTGTCAAGTAAGTTGTATTCTAGACAGTCCCCTTTTTTTAT-3′	Integrated DNA Technologies (Coralville, IA, USA) red: 178 A > G mutation blue: 189 G > A silent mutation
Sanger forward primer	5′-GACGACGAGGTACTGTCACC-3′	Integrated DNA Technologies (Coralville, IA, USA)
Sanger reverse primer	5′-CACCATGTGCTTCCC-3′	Integrated DNA Technologies (Coralville, IA, USA)

CrRNA: target-specific gRNA oligo, ssODN: knock-in single strand HDR donor template.

2.3. Polysome profiling

Cell suspension was treated with cycloheximide (CHX, Sigma-Aldrich, St. Louis, MO USA) at a concentration of 100 μg/ml for 20 min at 37 °C and 5 % CO_2. The harvested cells were then washed with ice-cold PBS containing CHX (100 μg/ml, Sigma-Aldrich, St. Louis, MO USA). Following this, the cells were lysed using a lysis buffer consisting of 0.1 M NaCl, 0.01 M Tris-HCl pH 7.6, 0.001 M EDTA, 0.1 % Triton X-100, 0.1 mM PMSF, 100 μM Sodium orthovanadate, 100 mM DTT, and 100 μg/ml CHX, along with 1X Proteases inhibitor mix (Roche Diagnostics, Basel, Switzerland). The lysate was cleared at 12,000 g for 10 min at 4 °C. An amount of the cytoplasmic lysate containing 1 mg of total protein was loaded onto 15–40 % sucrose gradients and centrifuged at 21,000 g at 4 °C for 2 h using an Optima L70 ultracentrifuge (Beckman, Brea, CA, USA), with slow acceleration and deceleration settings. After centrifugation, the tubes containing the sucrose gradients were prepared for analysis at the Gradient Station (Isco Teledyne, Lincoln, NE, USA) and measured for absorbance at 254 nm. Simultaneously, the samples were divided into 2 ml tubes, with fractions collection every minute. For data analysis and visualization of the polysome profile, TRACERDAQ STRIPCHART software was employed.

2.4. RNA isolation from polysomal profile fractions and Bioanalyzer analysis

For each sample, the RNA preparation involved combining 1/10 of each fraction to generate a pool of cytoplasmic RNA. This was then treated with 100 μg/ml proteinase K (Sigma-Aldrich, St. Louis, MO, USA) and 10 % SDS at 37 °C for 2 h. Following digestion, a phenol: chloroform solution (5:1, pH 4.7) was added to each sample and mixed thoroughly. Additionally, 5 M NaCl was added and mixed to promote phase separation. The samples were then centrifuged at 16,000 RCF for 5 min at 4 °C. The upper aqueous layer was subsequently transferred to a fresh tube, and 1 vol of isopropanol was added. The samples were thoroughly mixed and incubated overnight at −80 °C. Subsequently, centrifugation was performed at 16,000 RCF for 40 min at 4 °C, the supernatant was carefully removed, and the resulting pellet was washed with 70 % ethanol. Finally, the dried pellet was resuspended in RNase-free water to prepare the nucleic acid samples for further analysis. 28S/18S ratio was calculated analyzing RNAs with a Bioanalyzer 2100 system (Agilent Technologies, Santa Clara, CA, USA).

2.5. Ribosomes isolation

Ribosomes were purified as previously described [24]. Briefly, cells of two different WT and RPL5 I60V mutant clones were lysed in 10 mM Tris-HCl, pH 7.5, 10 mM NaCl, 3 mM $MgCl_2$ and 0.5 % (vol/vol) Nonidet P40 for 10 min on ice, and cytoplasmic lysates were collected upon centrifugation at 20,000 g for 10 min at 4 °C. After performing a 10 min incubation in protein synthesis master mix to achieve ribosomes run off from endogenous transcripts, lysates were loaded on a double cushion sucrose gradient with high salt/low salt conditions, to detach all ribosomes interactors. Ribosomes purification was achieved with a 15 h ultracentrifugation at 110,000 g_{av} at 4 °C. Ribosomal pellets were resuspended in ribosome solution and ribosome concentration was quantified by measuring the absorbance at 260 nm (A_{260}) in a NanoDrop® ND-1000 UV–Vis Spectrophotometer (ThermoFisher Scientific, Waltham, MA, USA) and applying the following formula: [mg/ml] of ribosomes = A_{260}/12.5.

2.6. Cell free translation assay

This assay was carried out as described in [24], with minor modifications. The transcript used in these assays was a pR-CrPV_IRES-F transcript, previously transcribed *in vitro* as indicated in [25].

2.7. Mass spectrometry (MS)-based proteomic analysis of purified ribosomes

Proteomics analysis was carried out essentially as previously described [26] with minor modifications. In particular, peptide separation was performed on a 75 μm 250 mm C18 analytical column (Aurora Generation 2, 1.6 μm particles, IonOpticks, Victoria, Australia). The chromatographic method consisted of a 120-minute multi-step gradient, increasing from 5 % to 41 % acetonitrile in 0.1 % formic acid, at a flow rate of 400 nL/min. Peptide and protein identification were performed with Mascot (v2.8), searching against the Uniprot human proteome database (March 2022 release), a custom sequence of the mutated RPL5 protein, an in-house contaminant database and their corresponding decoy versions for false discovery rate estimation. DDA results were merged using Proline software (v2.1). Validation and label-free quantification parameters followed those previously described [27]. Razor and specific peptides were used for quantification, except for RPL5 and its mutant form for which only strictly unique peptides were used. Mass spectrometry proteomics data have been deposited in the ProteomeXchange Consortium via the PRIDE repository under dataset identifier PXD064727 [28]. Statistical analysis was carried out using ProStaR 1.38.0 [29] following previously described method [30] with minor modifications, including an absolute log2 (fold change) threshold greater than 1.5 and an adjusted p-value (Benjamini-Hochberg correction) below 1 %.

2.8. RiboMethSeq and HydraPsiSeq analysis of rRNA modification profiles

rRNA was extracted from purified ribosomes with PureZOL™ (Bio-Rad, San Francisco, CA, USA) following manufacturer's protocol. Prior to proceeding further, rRNA quality was assessed with a Bioanalyzer RNA 6000 Nano assay (Agilent Technologies, Santa Clara, CA, USA): only samples with a RIN > 9 were selected for high throughput modification analyses. RiboMethSeq and HydraPsiSeq protocols used for quantification of rRNA modifications have been extensively described previously [31–36]. Both methods quantitatively measure protection of the modification-adjacent phosphodiester bond against chemically induced cleavage, which is alkaline hydrolysis for RiboMethSeq and hydrazine/aniline treatment for HydraPsiSeq. Analysis is performed simultaneously for all known modification sites (110 Nm and 107 ψ). In brief, rRNA is subjected to chemical treatment allowing to reveal resistant RNA phosphodiester bonds and the resulting fragments are converted to sequencing library using NEBNext Small RNA kit (NEB, Ipswich, MA, USA). Sequencing is performed in a single read SR50 mode, with the target value of ~10–15 mln of raw reads for RiboMethSeq and 20–25 mln for HydraPsiSeq. Bioinformatics treatment pipeline consists in trimming of the adapter sequence, alignment of the trimmed reads to the reference sequence and counting of 5′/3′-end for RiboMethSeq and 5′-ends only for HydraPsiSeq. Combined end-coverage profile is further used for calculation of MethScore and PsiScore, respectively.

2.9. Compounds preparation

For each compound, the optimal concentration range, to be tested on Jurkat cellular model, was determined based on available literature data. All the compounds (mentioned in Table 2) were purchased from Merck Life Science (Merck Millipore, Milan, Italy). Compounds solutions were prepared by dissolving them in specific solvents (water, ethanol, DMSO, as indicated in Table 2) to prepare concentrated stock solutions. These stocks were further diluted freshly for each experiment.

2.10. AlamarBlue™ assay

For each clone, 1×10^5 cells per well were seeded in a 96-well plate,

Table 2
List of tested compounds. For each drug (all Merck Millipore, Milan, Italy), the solvent used, along with the concentrations used in this study and relevant references, are indicated.

Compound	Vehicle	Higher Dose	IntermediateDose	Lower Dose	References
Homoharringtonine	DMSO	1 μM	0,1 μM	10 nM	[37]
Cytarabine	Water	1 μM	0,1 μM	0,01 μM	[38]
MNK1 Inhibitor4-Amino-5-(4-fluoroanilino) -pyrazolo[3,4-d]pyrimidine	Ethanol	100 μM	10 μM	1 μM	[39]
Resveratrol	DMSO	500 μM	100 μM	10 μM	[40]
Anisomycin	DMSO	10 μM	1 μM	0.1 μM	[41]
Metformin	Water	10 mM	–	1 mM	[42]
Hygromycin B	Water	750 μM	–	500 μM	–
Silvestrol	DMSO	1 nM	–	0.1 nM	–

in the presence of the drugs as indicated in Table 2, or in the presence of the solvent with the same final dilution as in the drug-treated wells (as a negative control). The plate was incubated at 37 °C, 5 % CO_2, and controlled humidity for 48 h. Alamarblue™ reagent (ThermoFisher Scientific, Waltham, MA, USA) was added directly into the culture media at a final concentration of 10 %, and the plate was incubated for 4 h at 37 °C, 5 % CO_2, after which fluorescence was measured in a Spark plate reader (TECAN, Männedorf, Switzerland).

2.11. Cell viability test

For each clone, 10^5 cells per well were seeded in a 96-well plate, in the presence of the drugs at the following concentration: the MNK1 inhibitor at 1 μM, metformin at 1 mM, silvestrol at 0.1 nM, homoharringtonine at 10 nM, anisomycin and cytarabine at 0.1 μM, resveratrol at 10 μM, and hygromycin B at 500 μM. Negative control were established using the solvent with the same final dilution as in the drug-treated wells. The plate was incubated at 37 °C, 5 % CO_2, and controlled humidity for 48 h. RealTime-Glo™ kit solution (containing NanoLuc® Luciferase and MT Cell Viability Substrate, Promega, Madison, WI, USA) was added at each well, following manufacturer's specification. The plate was then incubated at 37 °C with 5 % CO_2 for 72 h, and luminescence was recorded at specific time intervals in the Spark plate reader (TECAN, Männedorf, Switzerland).

2.12. Cytotoxicity and apoptosis

For each clone, 20,000 cells per well were seeded in a 96-well cell culture plate and treated with drugs at concentration reported in the previous paragraph and negative controls were established by seeding cells without drug treatment. The plate was then incubated at 37 °C, 5 % CO_2, and controlled humidity for 8 h or 24 h for apoptosis assessment, and 40 h for cytotoxicity analysis. Then, the ApoTox-Glo™ Triplex Assay (Promega, Madison, WI, USA) was used to assay cytotoxicity or apoptosis, following the manufacturer's instructions. Briefly, following incubation, a Viability/Cytotoxicity Reagent or Caspase-Glo® 3/7 Reagent were added to assess cytotoxicity or apoptosis, respectively. Plates were incubated for 30 min at room temperature, then fluorescence or luminescence measurements were taken using a Spark plate reader (TECAN, Männedorf, Switzerland). For fluorescence measurements, the wavelength sets were 485 nm excitation and 520 nm emission for cytotoxicity. For luminescence measurement, integration time was set to 1 s.

2.13. SUnSET assay and western blot analysis

To assess protein synthesis, the SUnSET assay was carried out as previously outlined [43]. For each clone, 10^5 cells per well were seeded in a 12-well cell culture plate and treated with drugs at the concentration reported in the previous paragraphs and negative controls were established by seeding cells without drug treatment. The plate was then placed in an incubator set at 37 °C, 5 % CO_2, and controlled humidity for 24 h. Cells were exposed to puromycin (1 μg/ml) for 10 min ("pulse") followed by two washes with ice-cold PBS. Subsequently, cells underwent a 50-minute "chase" period in fresh media at 37 °C with 5 % CO_2. Total proteins were extracted utilizing RIPA buffer (50 mM Tris-HCl pH 7.5, 150 mM NaCl, 1 % IGEPAL, 0.1 % SDS and protease inhibitor cocktail), and 30 μg of proteins were denatured and separated on a 10 % polyacrylamide gel, then transferred onto nitrocellulose membrane, and protein loading was assessed through stain-free technology (Bio-Rad, San Francisco, CA, USA). The membrane was then incubated overnight with the primary antibody [mouse anti-puromycin (12D10, Sigma-Aldrich, St. Louis, MO, USA, diluted 1:5000). After incubation with HRP- conjugated anti-mouse IgG antibody (Jackson Immunoresearch, Cambridge UK,) diluted 1:10000, the membrane blots were developed using the ChemiDoc Imaging System (Bio-Rad, San Francisco, CA, USA) and analyzed with Image Lab software.

2.14. Statistical analysis

Statistical analysis was performed using GraphPad Prism 8 statistical software. Statistical tests used and p-values are indicated in figure legends.

3. Results

3.1. Impact of I60V mutation on ribosome biogenesis and function

We selected I60V as a representative T-ALL–associated RPL5 mutation, since this substitution was previously identified in another T-ALL cell line derived from a pediatric patient (DND41) [4]. Indeed, I60 is located within the same functional region as other patient-derived mutations (Fig. 1A). RPL5 is assembled within nascent ribosomes in complex with RPL11 and 5S rRNA, in a structure called 5S ribonucleoprotein (5S-RNP). Even though the precise timing of incorporation of this complex in the large subunit during ribosome biogenesis is not clearly defined, it is known that it is a quite early event, occurring in the nucleolus (reviewed in [44]). On this premise, we reasoned that RPL5 I60V mutation could, in line of principle, impair the biogenesis of the large subunit, in terms of either RP or rRNA composition (Fig. 1A). To explore this specific issue, we generated a homozygous knock-in mutant model in Jurkat T-ALL cells and verified the genetic status by Sanger sequencing (Fig. 1B). We then adopted multiple approaches to study ribosome biogenesis. First, we confirmed by MS-based quantitative proteomic analysis the incorporation of the I60V RPL5 protein in cytoplasmic ribosomes of mutant cells (Fig. 1C). This approach demonstrated that RPL5 was the only ribosomal protein differentially abundant in ribosomal fractions from WT and mutant cells, with WT RPL5 significantly enriched in WT cells and I60V RPL5 significantly enriched in mutant cells (Fig. 1C). In addition, few non-ribosomal proteins were found differentially abundant in ribosomal preparations from WT and mutant cells (Table 3). Polysome profiling indicated a slight decrease in the 60S and 80S peaks in RPL5-I60V compared to RPL5-wt (Fig. 1D, E), mirrored by a non-significant reduction in 60S/40S ratio (Fig. 1F),

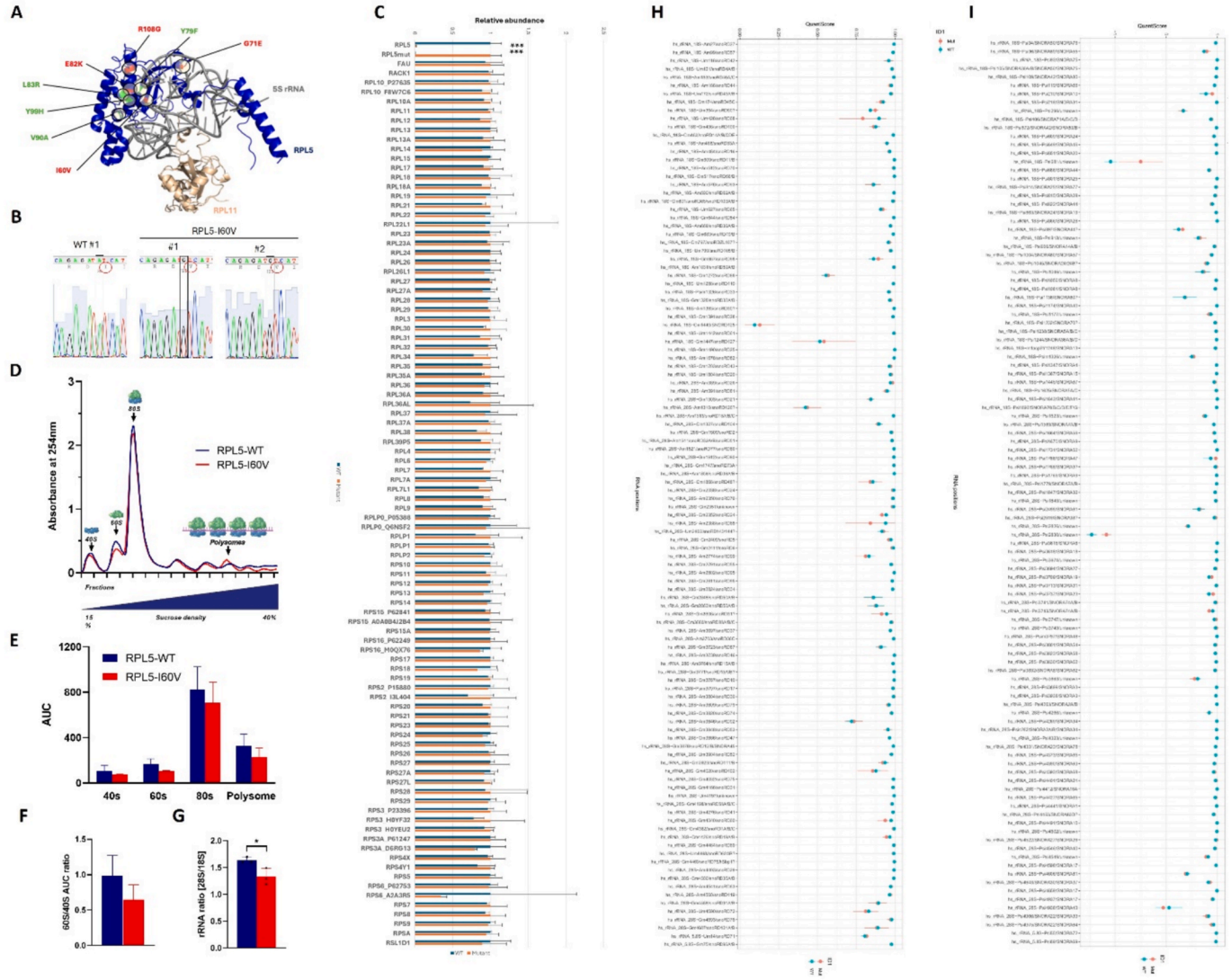

Fig. 1. Impact of RPL5 I60V mutation on ribosome biogenesis. (A) RPL5 structure within the 5S-RNP. RPL5 (in blue) assembled with RPL11 (in gold) and part of the 5S rRNA (in grey), from the PDB structure 4v6x. I60 as well as the residues found mutated in pediatric T-ALL (from https://www.stjude.cloud/) are highlighted in red, whereas the residues found mutated in other pediatric cancers are in green. (B) Sanger sequencing of Jurkat clones showing RPL5 wild-type or c.178A > G (p. I60V) mutation generated by CRISPR/Cas9. Black box: nucleotide substitution; red circle: amino acid substitution. (C) Relative abundance of the RPs detected in MS-based proteomic analysis of purified ribosomes from 2 wild type clones (WT) and 2 I60V mutant (Mutant) clones. Data represent the mean of three independent experiments; for each protein, the maximum mean abundance was set to 1. Error bars represent standard deviation. ***limma p-value < 0.001 in the statistical analysis of quantitative proteomics data (see Materials and methods section). (D) Representative polysome profiles obtained by the separation on 15–40 % sucrose-density gradients of cytoplasmic extracts from 2 wt and 2 RPL5 I60V clones. The average A_{254} values for each WT and mutant clone are shown in blue and red, respectively. (E) For each of the different samples, areas under the curve (AUC) were determined and plotted. (F) Ratio of 60S and 40S peak areas/total areas. (G) Ratio of 28S/18S total cytoplasmic rRNA, determined by Bioanalyzer. (H) RiboMethSeq analysis. Panel shows values of rRNA MethScore (QuantScore) for WT (blue) and RPL5 I60V cells (Mut, red). Analysis was performed for 2 wt and 2 mutant clones. The mean value is shown as a dot and error bar shows variability between two replicates. The majority of Nm sites are almost fully modified, while few show only partial methylation (MethScore < 0.75). Identity of the rRNA Nm site as well as associated C/D-box snoRNA are shown at the bottom. (I) HydraPsiSeq analysis. Panel shows values of rRNA PsiScore (QuantScore) for WT (blue) and RPL5 I60V cells (Mut, red). Analysis was performed for 2 wt and 2 mutant clones. The mean value is shown as a dot and error bar shows variability between two replicates. Three rRNA sites with negative PsiScore levels show higher cleavage compared to the neighboring nucleotides and thus are not modified even in the WT human cells. Identity of the rRNA Nm site as well as associated H/ACA-box snoRNA are shown at the bottom.

suggesting a quantitative effect of the RPL5 mutation on large subunit biogenesis. Consistent with this observation, we could report a decrease in the 28S/18S rRNA ratio determined on the rRNAs purified from total cytoplasmic RNA (Fig. 1G). Extensive rRNA modifications play an important role in the processing of rRNA itself, 2′-*O*-Methylation and pseudouridylation being the most frequent modifications on rRNAs [45]. We therefore performed an analysis of rRNA 2′-*O*-methylation and pseudouridylation profiles by RiboMethSeq [31] and HydraPsiSeq [32] protocols, respectively. Both methods have been fully optimized for quantitative assessment of the RNA modification level [33–36] and extensively used for analysis of rRNA modification dynamics. The results (Fig. 1H, I) clearly indicate that the I60V RPL5 mutation does not affect either modification.

We next evaluated the effect of the mutation on ribosomal function. Mutant cells showed an increase in puromycin incorporation in nascent peptides (Fig. 2A), indicating a more active protein synthesis. Consistently, we found that ribosomes purified from mutant cells had an intrinsic activity boosted by 50 % more, compared to WT (Fig. 2B), and this higher synthetic activity proved to be independent of the initiation mode (cap vs IRES). In keeping with a more active translation, we found

Table 3
List of ribosomal and non-ribosomal proteins differentially expressed in wild type (WT) or mutant (Mut) clones by MS-based quantitative proteomic analysis. In red background, proteins that are up-regulated in I60V-RPL5 mutant clones, in blue background the down regulated.

Protein Entry Name	Gene Name	Log_2 Fold Change (Mut vs WT)	p-value
RL5_mutI60V	RPL5mut	8,19	1,9E-06
Q16577_HUMAN	PTI-1	5,60	6,2E-04
ARL4C_HUMAN	ARL4C	3,44	5,8E-06
XPF_HUMAN	ERCC4	3,38	4,6E-06
H7C3W8_HUMAN	LRPPRC	2,80	1,6E-04
RL5_HUMAN	RPL5	-6,46	3,8E-06
NPC1_HUMAN	NPC1	-2,87	2,9E-05
ABCBA_HUMAN	ABCB10	-2,57	8,7E-05
ETFD_HUMAN	ETFDH	-1,71	3,3E-04
B3GN2_HUMAN	B3GNT2	-1,70	5,5E-04
TRI27_HUMAN	TRIM27	-1,53	1,2E-03

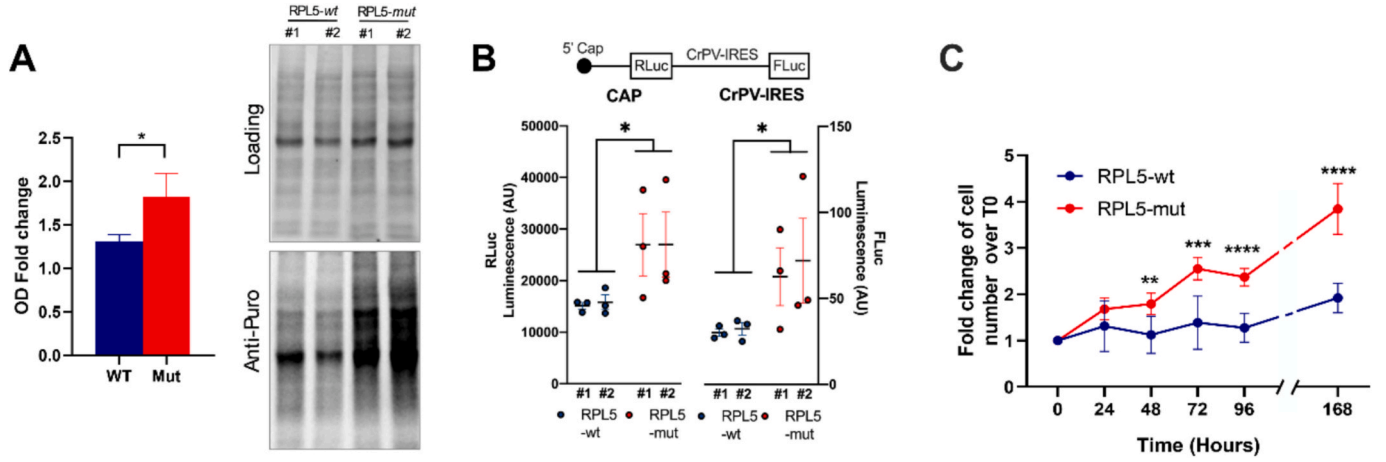

Fig. 2. Impact of RPL5 I60V mutation on ribosome function. (A) Cellular protein synthesis rate tested by SUnSET puromycin incorporation. Right: representative western blot. Left: normalized densitometric quantification of puromycin incorporation. Data are plotted as mean of fold change vs WT#1 ± SD. (B) Cell free translation efficiency of ribosomes purified from WT or I60V mutant clones, quantified as cap (Renilla Luciferase – Rluc luminescence) or CrPV IRES (Firefly Luciferase – Fluc luminescence)-mediated translation of a bicistronic Luciferase reporter mRNA. Luminescence is expressed in arbitrary units. Each dot represents the average of duplicate measurements. (C) Average proliferation curves over a 7 days-time span of WT and I60V mutant clones. Unless otherwise stated, experiments were performed in 3 biological replicates with 2 I60V and 2 wt clones. Statistical significance was calculated by *t*-test, with *p < 0.05, **p < 0.01, ***p < 0.001 and ****p < 0.0001.

that RPL5 mutant cells had a higher growth rate compared to WT, especially when cells reached a higher culture density (Fig. 2C).

3.2. *Impact of I60V mutation on the efficacy of compounds with diverse mechanisms of action*

Since our data indicated that the I60V mutation in RPL5 can significantly impact ribosome biogenesis, translation and, therefore, cellular proliferation, we next aimed to understand if the mutation could affect the effectiveness of drugs that target the translational machinery. Our interest was specifically focused on addressing whether the RPL5 mutation could, directly or indirectly, modulate the sensitivity of the cells to treatments. We therefore selected several drugs with different mechanisms of action on translation (ribosome biogenesis inhibitors, inhibitors of pathways upstream of protein synthesis, direct inhibitors of ribosome function). In addition, we added compounds used for T-ALL therapy, like cytarabine [46]. We tested the effect of these drugs on cellular metabolic activity, viability, protein synthesis and cell death in the WT or RPL5-I60V background. To assess their efficacy, we undertook an extensive literature review aimed at pinpointing optimal concentrations, in terms of cell growth inhibition, for our cellular model. These concentrations were selected as intermediate values within a wider spectrum, ranging from tenfold higher to tenfold lower concentrations (see Table 2). Since precise concentrations of hygromycin B and silvestrol were not readily available in the literature, a preliminary assessment was conducted to determine their effective concentration range (data not shown).

3.2.1. *Effect of the mutation on drug-mediated modulation of metabolic activity*

We first assessed the metabolic differences at the steady state for the cells harboring the two genotypes, finding a slight, non-statistically significant reduction in the I60V genotype (data not shown). We then defined the optimal drug concentration by evaluating the effect of drug treatments over 48 h on cellular metabolic activity/viability by AlamarBlue assay. Based on their effect, compounds can be divided into two groups (Fig. 3): one for which there is a dose/response effect (MNK1 inhibitor, metformin, silvestrol, anisomycin, cytarabine) and one for

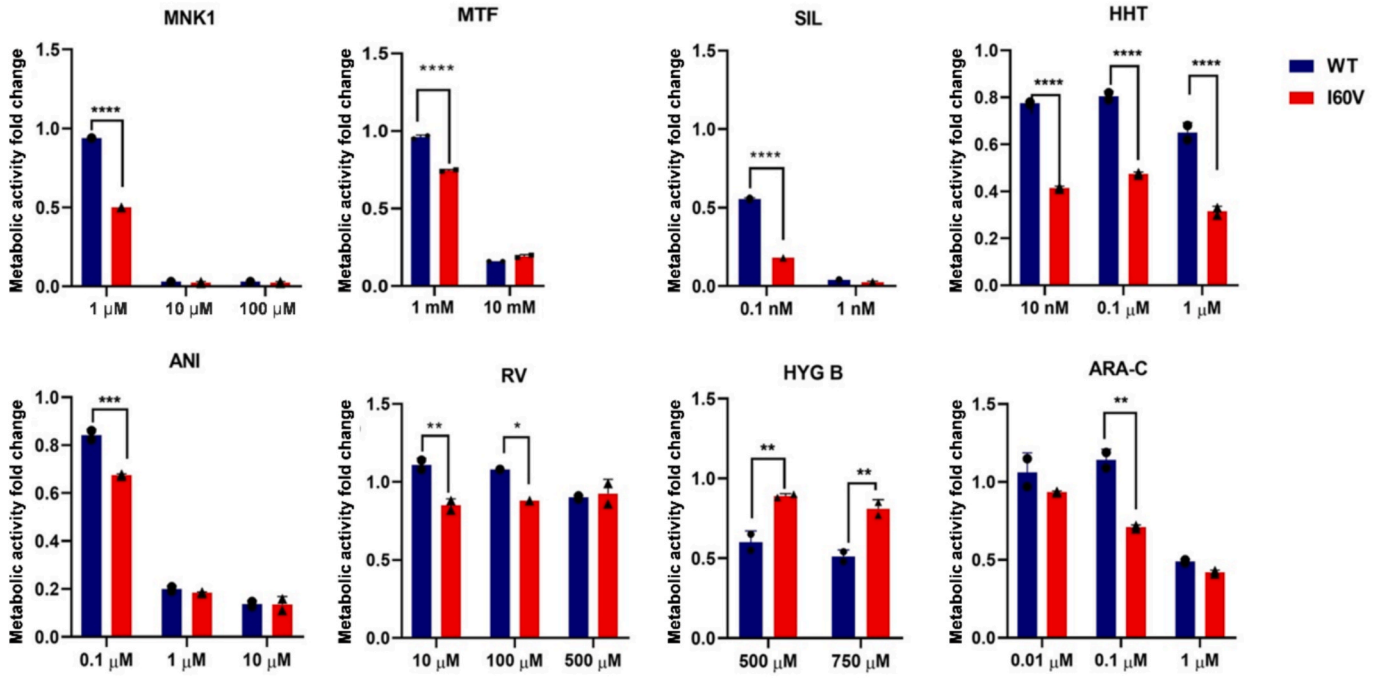

Fig. 3. Impact of drug treatment on cellular metabolic activity. The effect of the drugs on cellular metabolism was assessed by treating RPL5-WT (blue) and RPL5-I60V (red) clones with various drugs, primarily targeting translational machinery. Metabolic activity was evaluated, after a 48-hour treatment period, by AlamarBlue assay and data presented as fold change vs not treated sample. Graphs represent the average of two experiments run in duplicate. MNK1: MNK1 inhibitor; MTF: metformin; SIL: silvestrol; HHT: homoharringtonine; ANI: anisomycin; RV: resveratrol; HYG B: hygromycin B; ARA-C: cytarabine. Statistical significance was assessed by two-way ANOVA with Sidak's multiple comparisons test *p < 0.05, **p < 0.01, ***p < 0.001, ****p < 0.0001.

which the effect is very similar at the different doses tested (homoharringtonine, resveratrol, hygromycin B). This grouping is independent of the genetic background (WT or I60V) of the cells (Fig. 3). As illustrated in Fig. 3, RPL5-I60V clones generally demonstrated equal or higher sensitivity to the different treatments, compared to WT except for hygromycin B, for which RPL5-I60V clones exhibited resistance at the doses tested. Based on these results, we could define, in the tested range, the optimal concentration to be employed for further experiments, i.e., the lowest possible concentration at which significant differences in metabolism were observed between the mutant and wild-type (WT) cells. Specifically, the observed differences occurred at 1 μM for the MNK1 inhibitor, 1 mM for metformin, 0.1 nM for silvestrol, 10 nM for homoharringtonine, 0.1 μM for anisomycin, 10 μM for resveratrol, and 500 μM for hygromycin B. In contrast, for cytarabine, the most notable metabolic decrease occurred at the intermediate concentration of 0.1 μM, which was therefore chosen.

3.2.2. *Effect of the mutation on drug-mediated modulation of protein synthesis*

Because we tested various drugs known to inhibit ribosomal activity

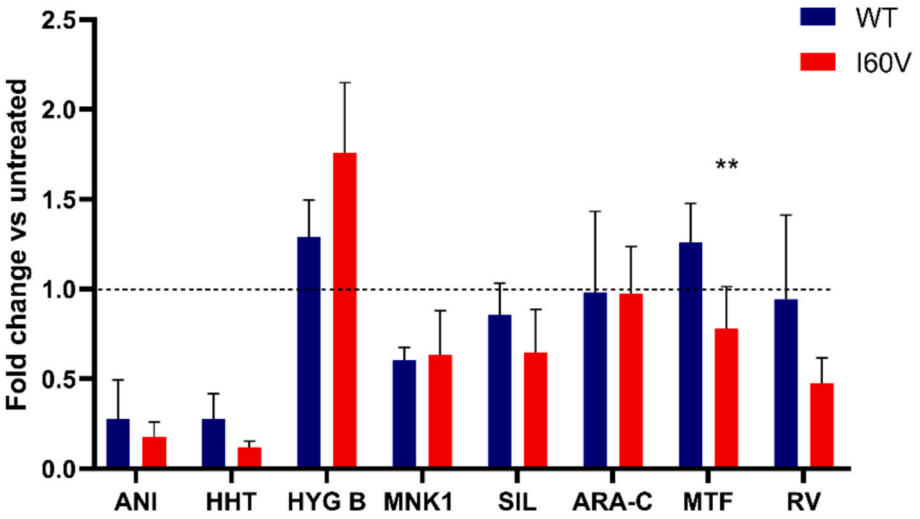

Fig. 4. Effect of different compounds on protein synthesis. SUnSET analysis depicts the puromycin incorporation in cells pre-treated for 24 h with the following drugs: anisomycin (ANI, 0.1 μM); homoharringtonine (HHT, 10 nM); hygromycin B (HYG B, 500 μM); MNK1 inhibitor (MNK1, 1 μM); silvestrol (SIL, 0.1 nM); cytarabine (ARA-C, 0.1 μM); metformin (MTF, 1 mM) and resveratrol (RV, 10 μM). The graph provides a quantitative representation of puromycin incorporation determined by western blot with anti-puromycin antibody, with results expressed as fold change relative to untreated cells + SD. Data represent the mean of two independent experiments. Statistical significance was assessed by *t*-test, **p < 0.01.

or protein synthesis, we aimed to evaluate how these drugs affect protein synthesis in cells with either wild-type RPL5 or the I60V mutation. To address this question, we performed non-radioactive labelling of newly synthesized proteins using puromycin incorporation (SUnSET) assay following a 24-hour drug treatment for both RPL5 WT and I60V clones.

Anisomycin and Homoharringtonine inhibited protein synthesis in both WT and mutant cells, with mutants showing greater sensitivity (Fig. 4). In contrast, hygromycin B did not suppress protein production in either cell type; instead, both showed increased protein expression relative to untreated controls, with mutants displaying stronger resistance (Fig. 4). Two translation initiation inhibitors, the MNK1 inhibitor and Silvestrol, reduced protein synthesis compared to controls, but effects were independent of the RPL5 genetic background. The antimetabolic agent cytarabine also had no significant effect on protein synthesis in either WT or I60V clones (Fig. 4). Metformin, which targets the mTOR pathway, caused stronger inhibition in mutant cells, while WT cells appeared resistant (Fig. 4). Similarly, resveratrol did not affect WT cells but induced a higher, though not significant, inhibition in I60V mutants (Fig. 4).

3.2.3. *Effect of the mutation on drug-mediated modulation of cytotoxicity*

Given the known association between changes in metabolic activity and cell viability [47], further assays were conducted to validate what

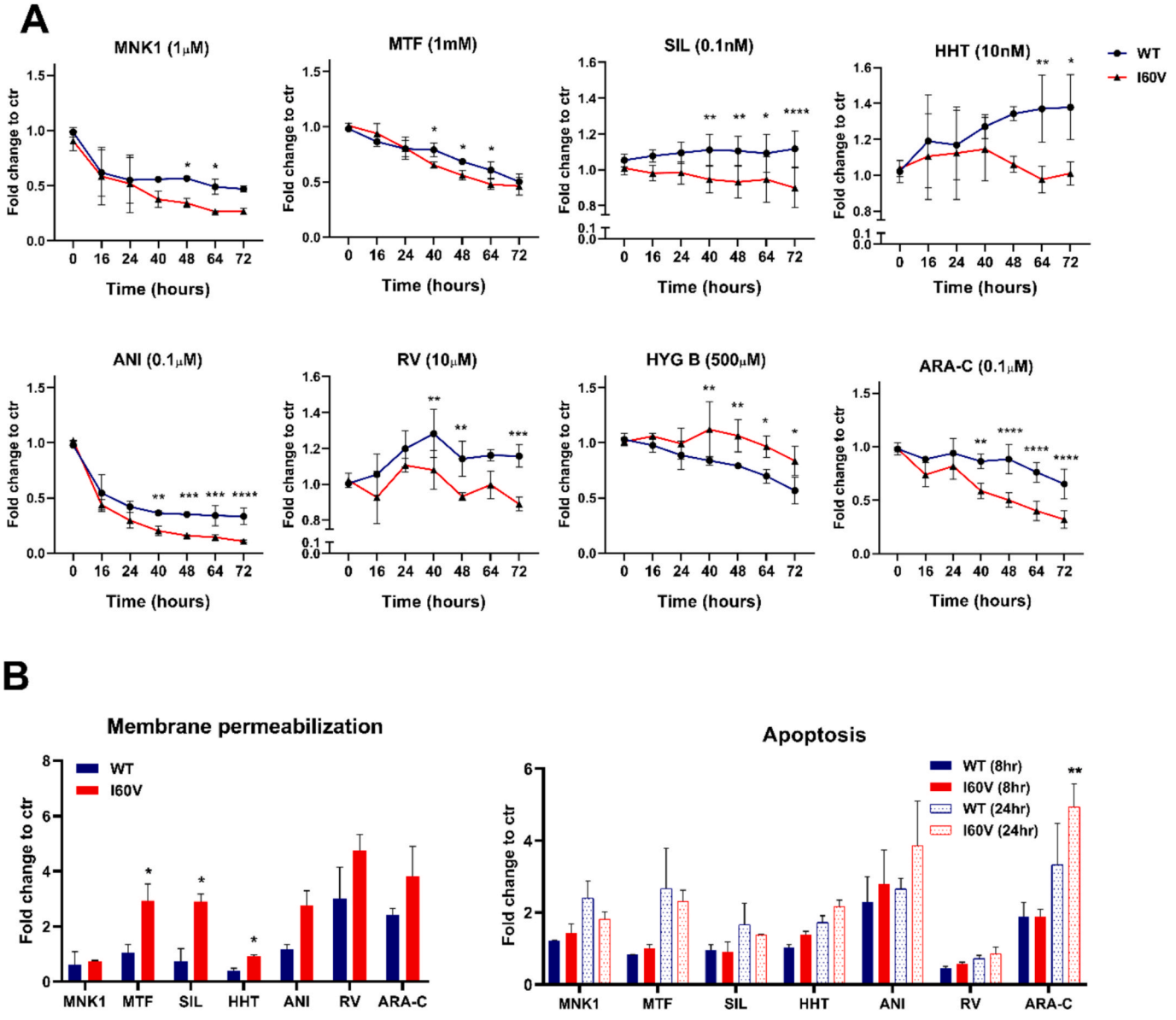

Fig. 5. Impact on cell viability, membrane permeabilization and apoptosis. (A) Cell viability was assessed with RPL5-WT (blue) and RPL5-I60V (red) clones using the RealTime-Glo™ assay (Promega). Cells were exposed to specified drug concentrations as indicated in figure. MNK1 inhibitor (MNK1, 1 μM), Metformin (MTF, 1 mM), silvestrol (SIL, 0.1 nM), homoharringtonine (HHT, 10 nM), anisomycin (ANI, 0.1 μM), resveratrol (RV, 10 μM), hygromycin B (HYG B, 500 μM), and cytarabine (ARA-C, 0.1 μM). Viability was monitored by measuring luminescence for 72 h. Experiments were conducted in triplicate for each drug, with appropriate controls and data are represented as fold change vs control (ctr) ± SD. Statistical significance was assessed by two-way ANOVA with Sidak's multiple comparisons test *p < 0.05, **p < 0.01, ***p < 0.001, ****p < 0.0001. (B) Cell membrane permeability and apoptosis were assessed in RPL5-WT (blue) and RPL5-I60V (red) clones using the ApoTox-Glo™ assay (Promega). Cells were exposed to specified drug concentrations, consistent with those used for cell viability assays, for 40 h to assess dead cell protease activity (readout of membrane permeabilization) and for 8 and 24 h to assess apoptosis. Data represent the mean of two independent experiments run in duplicate and are expressed as fold change vs control (ctr) ± SD. Statistical significance was assessed by two-way ANOVA with Sidak's multiple comparisons test *p < 0.05, **p < 0.01, ***p < 0.001, ****p < 0.0001.

reported in the previous paragraphs, with the aim to evaluate the drugs' efficacy in inducing cytotoxic effects in both RPL5-WT and RPL5-I60V clones. Optimal concentrations for viability assays were determined for each drug, based on their demonstrated efficacy in the metabolic assays (Fig. 3), and are reported in Fig. 5A. Cells were treated for 72 h, and, within this time frame, viability was assessed at various time points to ensure a comprehensive evaluation of the drugs' effects. As shown in Fig. 5A, drugs impacted cell viability in both RPL5-WT and RPL5-I60V backgrounds, but most drugs began to exhibit different and significant effects only after 40 h since treatment start. In general, two distinct effects of the treatments on cells could be observed, regardless of the RPL5 genotype. Specifically, a reduction in the number of viable cells was induced by the MNK1 inhibitor, metformin, anisomycin, hygromycin B, and cytarabine. In contrast, stabilization of cell numbers was observed with silvestrol, homoharringtonine, and resveratrol. MNK1 inhibitor and anisomycin showed the same trend (a high decrease after 16 h and then a constant decrease in the number of viable cells) on both wild type and mutant cells, with the latter showing higher sensitivity. In contrast, metformin, hygromycin B, and cytarabine demonstrated a comparatively moderate and temporally stable effect on the number of viable cells. While metformin elicited minimal RPL5-dependent differences, hygromycin B and cytarabine induced more pronounced effects. Notably, I60V clones exhibited greater resistance to hygromycin B treatment compared to wild-type clones. The effect of silvestrol, resveratrol and homoharringtonine was overall modest, with mutant clones showing no differences in the number of viable cells in treated versus untreated samples, whereas wild-type clones exhibited a modest increase.

A comprehensive evaluation of treatment efficacy was conducted, considering the heightened sensitivity of RPL5-I60V cells to most tested compounds. However, due to the consistently diminished response of RPL5-I60V clones to hygromycin B across metabolic/ viability, and protein synthesis assays, this compound was excluded from subsequent experiments. Utilizing the ApoTox-Glo™ assay, we addressed the toxic outcome upon treatment, thereby providing insights into the type of cellular response elicited by the different compounds. In fact, this assay is based on the use of a cell-impermeant substrate, to measure the loss of membrane integrity (generally associated to necrosis or other death programs) and of Caspase 3 and 7 substrates, to measure the activation and finalization of pro-apoptotic programs upon treatment. The choice of the time points for the assessment of apoptosis and membrane integrity (i.e. 8/24 h and 40 h respectively, Fig. 5B) was based on the results in the viability curve assays (Fig. 5A), and on the type of readout (an early event in apoptosis, i.e. caspase activation, as opposed to an endpoint event, i.e. membrane permeabilization). In our investigation of MNK inhibition, we observed induction of apoptosis without significant differences in membrane permeability between wild-type (WT) and RPL5-I60V mutant cells. Metformin treatment resulted in a marked membrane permeabilization in I60V mutants, while apoptosis levels remained comparable across genotypes, suggesting activation of apoptosis independent of genotype-specific differences. Silvestrol had minimal impact on WT cells, showing no effect on membrane integrity and only a slight increase in apoptosis at 24 h. In contrast, I60V mutant cells exhibited slight caspase activation and elevated membrane permeabilization following silvestrol treatment. I60V mutants treated with homoharringtonine displayed low, but significantly higher membrane permeabilization compared to WT cells, and higher apoptosis relative to untreated controls, with no differences in terms of RPL5 genetic background. Anisomycin produced pronounced effects on both genotypes, with a stronger impact on I60V mutants, reflected in enhanced apoptosis and membrane permeabilization. Resveratrol induced membrane permeabilization in both WT and mutant cells, with a more substantial effect in I60V mutants, though apoptosis activation remained minimal in both. Finally, cytarabine treatment led to greater effect on membrane permeabilization in mutant cells, with apoptosis observed at both time points and significantly elevated in I60V mutants at 24 h.

4. Discussion

First proposed over two decades ago [48], the concept of ribosomal heterogeneity as a regulator of protein synthesis has since gained substantial support in both physiological and pathological settings. Current evidence suggests that variations in ribosome composition—and consequently, structure—can drive functional specialization, enabling precise control of mRNA translation independently of transcription [23,49–52]. In pathology, ribosome diversity arising from aberrant RP sequence has been demonstrated to have functional repercussions on protein synthesis. It is, for instance, the case for RPL9 L20P in Diamond Blackfan Anemia, a ribosomopathy [26], or of RPL10 R98S in pediatric T-ALL [53]. In T-ALL, RPL10 mutations have been associated to altered translation, resulting in the rewiring of metabolic and stress response pathways [53–55]. In addition to the RPL10 R98S mutation—the most common and best characterized RP mutation driving disease in pediatric T-ALL—somatic mutations in RPL5 have also been reported, with missense variants being the most prevalent [56]. To investigate the role of RPL5 I60V missense mutation in ribosomal function within the context of T-ALL, we generated knock-in mutants in Jurkat cells, a pediatric T-ALL-derived cell line. This specific cellular model was chosen as it is widely used to study the molecular mechanisms underlying this disease, as well as to develop and test therapies in the context of leukemia. RPL5 is a structural part of the central protuberance of the large subunit of the ribosome, that is involved in the functional interconnection between the decoding center in the 40S and the peptidyl transferase center in the 60S [57]. Thus, mutations in RPL5 can potentially alter ribosome translational activity. In addition to its structural role in the ribosome, RPL5 is critically involved in pre-rRNA processing and ribosome biogenesis, and sequence alterations may disrupt these functions as well [58]. We began our work by assessing the impact of the I60V mutation on ribosome biogenesis and function. Our analyses revealed that the mutation slightly impaired the biogenesis of the 60S ribosomal subunit. Mature ribosomes purified under high-stringency conditions from both wild-type (WT) and RPL5 mutant clones showed no compositional differences, apart from the I60V substitution. This included ribosomal protein content as well as site-specific rRNA modifications, specifically pseudouridylation and 2′-O-methylation, the two most abundant modifications in rRNAs [45]. Noteworthy, despite purifying ribosomes in highly stringent conditions, the MS analysis highlighted a differential enrichment in few non-ribosomal proteins, namely PTI-1, ARL4C, ERCC4, LRPPRC, NPC1, ABCB10, ETFDH, B3GNT2, and TRIM27 (Table 3). These proteins were present in much lower amounts than ribosomal proteins in the analyzed samples (several hundred times less abundant than ribosomal proteins by comparing iBAQ values). Among all these proteins, an effect on mRNA translation was previously reported only for PTI-1, whose expression has been associated to RPL5 and RPL4 [59]. Despite involving a single amino acid change, the functional impact of the I60V substitution within ribosomes was striking. Ribosomes incorporating the I60V-RPL5 substitution displayed a pronounced increase in intrinsic protein synthesis activity, regardless of whether translation was initiated through the 5′ cap or an IRES. This single amino acid change in RPL5 thus enhances ribosomal translational efficiency, supporting the notion that structural alterations can drive functional specialization [60]. This enhanced translational capacity was accompanied by a faster proliferation rate in mutant cells, suggesting a growth advantage conferred by the mutation, especially in stressing conditions of higher cellular density. To our knowledge, this is the first report of a RP mutant being incorporated into ribosomes, resulting in enhanced translational efficiency.

Based on these first results, we asked ourselves whether mutant cells could be differentially affected by treatment with compounds targeting ribosomes or, more in general, the translational machinery. Indeed, the localization of RPL5-I60V in the central protuberance of ribosomes could potentially influence sensitivity to several ribosome-targeting antibiotics, including homoharringtonine, hygromycin B, and

anisomycin (all targeting the A site in the peptidyl transferase center). Leukemia cells heavily rely on cap-dependent translation via hyperactivation of signaling converging on eIF4A and eIF4E [61,62]. Since the RPL5-I60V mutation enhances translation rates, we hypothesized that these cells may exhibit heightened sensitivity to inhibitors of protein synthesis, like an inhibitor mitogen-activated protein kinase interacting kinase 1 (MNK1) [63], which targets phosphorylation of translation initiation factor 4E (eIF4E), and silvestrol, which targets eIF4A [61]. Moreover, we selected drugs targeting the mTOR signaling pathways, such as resveratrol [64] and metformin [65,66], which has also been shown to induce endoplasmic reticulum stress and inhibit the unfolded protein response (UPR) in leukemia cells [67]. For some of these compounds, prior use in experimental cancer therapies is reported (e.g. NCT01324180 for metformin; NCT00675350 for homoharringtonine, NCT00920803 for resveratrol, from https://www.clinicaltrials.gov). Additionally, we included cytarabine, a cornerstone chemotherapeutic agent in acute leukemia [68]. With the exception of cytarabine, all the tested compounds are expected to inhibit protein synthesis, albeit through distinct mechanisms as mentioned above. Indeed, our data show that only a subset of them—anisomycin, homoharringtonine, silvestrol, and the MNK1 inhibitor—was able to reduce protein synthesis to some extent in both genetic contexts. In contrast, metformin and resveratrol were effective only in the mutant background, suggesting that hyperactivated protein synthesis in RPL5-I60V cells may increase their reliance on this process. Furthermore, and in line with the metabolic data, mutant cells displayed even greater resistance to hygromycin B compared to WT.

When assessing the impact of the mutation on compound-mediated inhibition of cellular metabolic activity, we observed a bimodal response. Several drugs—such as silvestrol, anisomycin, MNK1 inhibitor, cytarabine, metformin, homoharringtonine, and resveratrol—exhibited greater efficacy in RPL5-I60V clones compared to RPL5-WT. In contrast, hygromycin B was less effective in RPL5-I60V cells. These findings suggest that the RPL5 mutation alone does not confer a general increase in resistance or sensitivity. Rather, drug-specific mechanisms of action, along with additional factors such as cellular uptake, metabolism, or clearance, likely contribute to the differential responses observed. In addition, while differential sensitivity to some compounds—such as homoharringtonine and hygromycin B—was evident across the entire tested concentration range, for most drugs it was restricted to the lower concentrations. This suggests that the mutation modulates sensitivity rather than producing an all-or-none effect.

Most drugs exhibited a significant impact on cell viability, in line with findings from the metabolic assays. While some compounds—such as silvestrol, homoharringtonine, and resveratrol—did not alter the overall number of viable cells over time (indicating a balance between the number of cycling, resting and dying cells), others—including the MNK1 inhibitor, metformin, anisomycin, hygromycin, and cytarabine—led to a marked reduction in cell number as early as 16 h after treatment initiation, suggesting the activation of cell death pathways. It worth underscoring, however, that the effect on cellular viability was, in most cases, genotype-dependent, with the I60V mutants being generally more sensitive compared to WT RPL5 genotypes. Consistently with the findings on cellular metabolism and protein synthesis inhibition, the only exception was represented by hygromycin B, for which mutant cells appeared to be more resistant compared to the WT genotype. Dependent of the treatment, we observed the activation of different cell death pathways. Most compounds, except for the MNK1 inhibitor and homoharringtonine, determined an increase in cytoplasmic membrane permeability at the second day of treatment, which was more evident in mutant cells than in wild type. Increased membrane permeability occurs in multiple cell death mechanisms, including necrosis, late apoptosis, and others, but the assays used herein do not allow for discriminating between them [69]. In addition, some treatments tuned up the apoptotic pathway, with a clear effect after 16 h except for silvestrol and resveratrol. Mutant cells appeared to activate apoptosis to equal or higher levels compared to RPL5-WT cells. Our data are in line with previous literature showing a proapoptotic effect on leukemia cells of the different compounds in the tested concentration ranges ([70] ARA-C; [71] ANI; [72] HHT; [73] MTF; [74] MNK1), but based on available data it is not possible to define whether other secondary death mechanisms are elicited by the tested compounds.

A main limitation of this study is the use of a single cell line. While some experiments were performed on purified ribosomes—thus bypassing potential cell-specific background effects—many others relied on cell-based assays and were therefore influenced by cell line–specific characteristics. This includes the drug testing, where the observed results may reflect cellular features unrelated to the mutation of interest. In addition, although our data suggest a ribosome-centered effect of the I60V mutation, we cannot exclude the possibility that this mutation also affects ribosome-independent functions of RPL5. These may include its role as an activator of ribosomal stress responses via the 5S-ribonucleoparticles (5S-RNPs) [75] as well as its involvement in transcriptional regulation [15,76]. Future studies will be needed to address this question and to investigate the potential of combination therapies using the tested compounds with distinct mechanisms of action, whose efficacy appears enhanced in the context of RPL5-I60V.

4.1. Conclusions

This study opens a new perspective in the treatment of those cancers which bear alterations in ribosomes or in the translational machinery, shedding light on the potential of ribosomal proteins as therapeutic targets for the development of increasingly personalized, more effective and less toxic therapies.

Funding sources

This work was supported by the Italian Foundation for Cancer Research (AIRC) [grant number MFAG-19941], Fondazione Umberto Veronesi (Fellowship to DP and MP), Beneficentia Stiftung and the Pallotti Legacy for Cancer Research. The proteomic experiments were partially supported by ANR under projects ProFI (Proteomics French Infrastructure, ANR-10-INBS-08) and GRAL, a program from the Chemistry Biology Health (CBH) Graduate School of University Grenoble Alpes (ANR-17-EURE-0003).

CRediT authorship contribution statement

Lorenza Bacci: Writing – original draft, Visualization, Formal analysis. **Daniela Pollutri:** Investigation, Formal analysis, Data curation. **Israt Jahan Ripa:** Writing – original draft, Investigation, Formal analysis, Data curation. **Michael D'Andrea:** Visualization, Investigation, Formal analysis, Data curation. **Virginie Marchand:** Writing – original draft, Visualization, Investigation, Formal analysis, Data curation. **Yuri Motorin:** Writing – original draft, Visualization, Investigation, Formal analysis, Data curation. **Anne-Marie Hesse:** Writing – original draft, Visualization, Investigation, Formal analysis, Data curation. **Yohann Couté:** Writing – original draft, Visualization, Investigation, Formal analysis, Data curation. **Kamil Filipek:** Visualization, Investigation, Formal analysis, Data curation. **Marianna Penzo:** Writing – original draft, Visualization, Supervision, Funding acquisition, Conceptualization.

Declaration of competing interest

The authors declare that they have no known competing financial interests or personal relationships that could have appeared to influence the work reported in this paper.

Acknowledgments

This article/publication is based upon work from COST Action TRANSLACORE CA21154, supported by COST (European Cooperation in Science and Technology). MP warmly thanks Professor Lorenzo Montanaro and his research group for continuous discussion on the project, and Prof. Kenneth B. Marcu for critical reading of the final draft of the manuscript.

Data availability

Data are accessible to reviewers based on the information present in the manuscript, and will be made freely accessible to everyone upon publication.

References

[1] F. Gianni, L. Belver, A. Ferrando, The genetics and mechanisms of T-cell acute lymphoblastic leukemia, Cold Spring Harb. Perspect. Med. 10 (2020), https://doi.org/10.1101/CSHPERSPECT.A035246.
[2] D. Bongiovanni, V. Saccomani, E. Piovan, Aberrant signaling pathways in T-cell acute lymphoblastic leukemia, Int. J. Mol. Sci. 18 (2017) 1904, https://doi.org/10.3390/IJMS18091904.
[3] Y. Liu, J. Easton, Y. Shao, J. Maciaszek, Z. Wang, M.R. Wilkinson, K. McCastlain, M. Edmonson, S.B. Pounds, L. Shi, X. Zhou, X. Ma, E. Sioson, Y. Li, M. Rusch, P. Gupta, D. Pei, C. Cheng, M.A. Smith, J.G. Auvil, D.S. Gerhard, M.V. Relling, N. J. Winick, A.J. Carroll, N.A. Heerema, E. Raetz, M. Devidas, C.L. Willman, R. C. Harvey, W.L. Carroll, K.P. Dunsmore, S.S. Winter, B.L. Wood, B.P. Sorrentino, J. R. Downing, M.L. Loh, S.P. Hunger, J. Zhang, C.G. Mullighan, The genomic landscape of pediatric and young adult T-lineage acute lymphoblastic leukemia, Nat. Genet. 49 (2017) 1211–1218, https://doi.org/10.1038/NG.3909.
[4] K. De Keersmaecker, Z.K. Atak, N. Li, C. Vicente, S. Patchett, T. Girardi, V. Gianfelici, E. Geerdens, E. Clappier, M. Porcu, I. Lahortiga, R. Lucà, J. Yan, G. Hulselmans, H. Vranckx, R. Vandepoel, B. Sweron, K. Jacobs, N. Mentens, I. Wlodarska, B. Cauwelier, J. Cloos, J. Soulier, A. Uyttebroeck, C. Bagni, B. A. Hassan, P. Vandenberghe, A.W. Johnson, S. Aerts, J. Cools, Exome sequencing identifies mutation in CNOT3 and ribosomal genes RPL5 and RPL10 in T-cell acute lymphoblastic leukemia, Nat. Genet. 45 (2013) 186–190, https://doi.org/10.1038/ng.2508.
[5] G. Tzoneva, A. Perez-Garcia, Z. Carpenter, H. Khiabanian, V. Tosello, M. Allegretta, E. Paietta, J. Racevskis, J.M. Rowe, M.S. Tallman, M. Paganin, G. Basso, J. Hof, R. Kirschner-Schwabe, T. Palomero, R. Rabadan, A. Ferrando, Activating mutations in the NT5C2 nucleotidase gene drive chemotherapy resistance in relapsed ALL, Nat. Med. 19 (2013) 368, https://doi.org/10.1038/NM.3078.
[6] S. Rao, S.Y. Lee, A. Gutierrez, J. Perrigoue, R.J. Thapa, Z. Tu, J.R. Jeffers, M. Rhodes, S. Anderson, T. Oravecz, S.P. Hunger, R.A. Timakhov, R. Zhang, S. Balachandran, G.P. Zambetti, J.R. Testa, A.T. Look, D.L. Wiest, Inactivation of ribosomal protein L22 promotes transformation by induction of the stemness factor, Lin28B, Blood 120 (2012) 3764–3773, https://doi.org/10.1182/BLOOD-2012-03-415349.
[7] S.O. Sulima, I.J.F. Hofman, K. De Keersmaecker, J.D. Dinman, How ribosomes translate cancer, Cancer Discov. 7 (2017) 1069–1087, https://doi.org/10.1158/2159-8290.CD-17-0550.
[8] K.M. Goudarzi, M.S. Lindström, Role of ribosomal protein mutations in tumor development (Review), Int. J. Oncol. 48 (2016) 1313–1324, https://doi.org/10.3892/IJO.2016.3387.
[9] I. Oršolić, S. Bursać, D. Jurada, I. Drmić Hofman, Z. Dembić, J. Bartek, I. Mihalek, S. Volarević, Cancer-associated mutations in the ribosomal protein L5 gene dysregulate the HDM2/p53-mediated ribosome biogenesis checkpoint, Oncogene 39 (2020) 3443–3457, https://doi.org/10.1038/s41388-020-1231-6.
[10] L. Fancello, K.R. Kampen, I.J.F. Hofman, J. Verbeeck, K. De Keersmaecker, The ribosomal protein gene RPL5 is a haploinsufficient tumor suppressor in multiple cancer types, Oncotarget 8 (2017) 14462–14478, https://doi.org/10.18632/oncotarget.14895.
[11] J. Kang, N. Brajanovski, K.T. Chan, J. Xuan, R.B. Pearson, E. Sanij, Ribosomal proteins and human diseases: molecular mechanisms and targeted therapy, Signal Trans. Targeted Therapy 6 (1) (2021) 1–22, https://doi.org/10.1038/s41392-021-00728-8.
[12] T.I. Odintsova, E.C. Müller, A.V. Ivanov, T.A. Egorov, R. Bienert, S.N. Vladimirov, S. Kostka, A. Otto, B. Wittmann-Liebold, G.G. Karpova, Characterization and analysis of posttranslational modifications of the human large cytoplasmic ribosomal subunit proteins by mass spectrometry and Edman sequencing, J. Protein Chem. 22 (2003) 249–258, https://doi.org/10.1023/A:1025068419698.
[13] K.H. Olausson, M. Nistér, M.S. Lindström, p53 -dependent and -independent nucleolar stress responses, Cells 1 (2012) 774–798, https://doi.org/10.3390/CELLS1040774.
[14] N.F. DeCleene, E. Asik, A. Sanchez, C.L. Williams, E.B. Kabotyanski, N. Zhao, N. Chatterjee, K. Miller, Y.H. Wang, A.A. Bertuch, RPS19 and RPL5, the most commonly mutated genes in Diamond Blackfan anemia, impact DNA double-strand break repair, BioRxiv (2024), https://doi.org/10.1101/2024.10.10.617668.
[15] G. Rambaldelli, L. Bacci, D. Pollutri, K. Filipek, M. Penzo, Master of disguise: ribosomal protein L5 beyond translation, Biochimie (2025), https://doi.org/10.1016/J.BIOCHI.2025.03.009.
[16] K. Norris, T. Hopes, J.L. Aspden, Ribosome heterogeneity and specialization in development, Wiley Interdiscip. Rev.: RNA 12 (2021), https://doi.org/10.1002/WRNA.1644.
[17] S. Ramalho, A. Dopler, W.J. Faller, Ribosome specialization in cancer: a spotlight on ribosomal proteins, NAR Cancer 6 (2024), https://doi.org/10.1093/NARCAN/ZCAE029.
[18] A. Kochavi, D. Lovecchio, W.J. Faller, R. Agami, Proteome diversification by mRNA translation in cancer, Mol. Cell 83 (2023) 469–480, https://doi.org/10.1016/J.MOLCEL.2022.11.014.
[19] H. Inaba, C.G. Mullighan, Pediatric acute lymphoblastic leukemia, Haematologica 105 (2020) 2524–2539, https://doi.org/10.3324/HAEMATOL.2020.247031.
[20] M.W. Lato, A. Przysucha, S. Grosman, J. Zawitkowska, M. Lejman, The new therapeutic strategies in pediatric T-cell acute lymphoblastic leukemia, Int. J. Mol. Sci. 22 (2021), https://doi.org/10.3390/IJMS22094502.
[21] A.N. Guerrieri, C.M. Hattinger, F. Marchesini, M. Melloni, M. Serra, T. Ibrahim, M. Penzo, The interplay between the MYC oncogene and ribosomal proteins in osteosarcoma onset and progression: potential mechanisms and indication of candidate therapeutic targets, Int. J. Mol. Sci. 25 (2024), https://doi.org/10.3390/IJMS252212031.
[22] K. Filipek, M. Penzo, Ribosomal rodeo: wrangling translational machinery in gynecologic tumors, Cancer Metastasis Rev. 44 (2025), https://doi.org/10.1007/S10555-024-10234-2.
[23] V. Gelfo, G. Venturi, F. Zacchini, L. Montanaro, Decoding ribosome heterogeneity: a new horizon in cancer therapy, Biomedicines 12 (2024), https://doi.org/10.3390/BIOMEDICINES12010155.
[24] M. Penzo, D. Carnicelli, L. Montanaro, M. Brigotti, A reconstituted cell-free assay for the evaluation of the intrinsic activity of purified human ribosomes, Nat. Protoc. 11 (2016) 1309–1325, https://doi.org/10.1038/NPROT.2016.072.
[25] M. Penzo, L. Rocchi, S. Brugiere, D. Carnicelli, C. Onofrillo, Y. Coute, M. Brigotti, L. Montanaro, Human ribosomes from cells with reduced dyskerin levels are intrinsically altered in translation, FASEB J. 29 (2015) 3472–3482, https://doi.org/10.1096/FJ.15-270991.
[26] M. Lezzerini, M. Penzo, M.F. O'Donohue, C.M. Dos Santos Vieira, M. Saby, H.L. Elfrink, I.J. Diets, A.M. Hesse, Y. Couté, M. Gastou, A. Nin-Velez, P.G.J. Nikkels, A. N. Olson, E. Zonneveld-Huijssoon, M.C.J. Jongmans, G.J. Zhang, M. Van Weeghel, R.H. Houtkooper, M.W. Wlodarski, R.P. Kuiper, M.B. Bierings, J. Van Der Werff Ten Bosch, T. Leblanc, L. Montanaro, J.D. Dinman, L. Da Costa, P.E. Gleizes, A.W. MacInnes, Ribosomal protein gene RPL9 variants can differentially impair ribosome function and cellular metabolism, Nucleic Acids Res 48 (2020) 770. https://doi.org/10.1093/NAR/GKZ1042.
[27] O. Filhol, A.M. Hesse, A.P. Bouin, C. Albigès-Rizo, F. Jeanneret, C. Battail, D. Pflieger, C. Cochet, CK2β is a gatekeeper of focal adhesions regulating cell spreading, Front. Mol. Biosci. 9 (2022), https://doi.org/10.3389/FMOLB.2022.900947/PDF.
[28] Y. Perez-Riverol, A. Csordas, J. Bai, M. Bernal-Llinares, S. Hewapathirana, D. J. Kundu, A. Inuganti, J. Griss, G. Mayer, M. Eisenacher, E. Pérez, J. Uszkoreit, J. Pfeuffer, T. Sachsenberg, Ş. Yilmaz, S. Tiwary, J. Cox, E. Audain, M. Walzer, A. F. Jarnuczak, T. Ternent, A. Brazma, J.A. Vizcaíno, PRIDE The database and related tools and resources in, Improving support for quantification data, Nucleic Acids Res. 47 (2019) (2019) D442–D450, https://doi.org/10.1093/NAR/GKY1106.
[29] S. Wieczorek, F. Combes, C. Lazar, Q.G. Gianetto, L. Gatto, A. Dorffer, A.M. Hesse, Y. Couté, M. Ferro, C. Bruley, T. Burger, DAPAR & ProStaR: software to perform statistical analyses in quantitative discovery proteomics, Bioinformatics 33 (2017) 135–136, https://doi.org/10.1093/BIOINFORMATICS/BTW580.
[30] P. Poteaux, A. Parpinel, C. Ripoll, A. Sarrazin, R. Galinier, S. Brugière, Y. Couté, L. Mourey, P.C. Hanington, B. Gourbal, L. Maveyraud, D. Duval, The structural features and immunological role of biomphalysins in the snail Biomphalaria glabrata, PLoS Pathog. 21 (2025) e1013225, https://doi.org/10.1371/JOURNAL.PPAT.1013225.
[31] V. Marchand, F. Blanloeil-Oillo, M. Helm, Y. Motorin, Illumina-based RiboMethSeq approach for mapping of 2′-O-Me residues in RNA, Nucl. Acids Res. 44 (2016) e135, https://doi.org/10.1093/nar/gkw547.
[32] V. Marchand, F. Pichot, P. Neybecker, L. Ayadi, V. Bourguignon-Igel, L. Wacheul, D.L.J. Lafontaine, A. Pinzano, M. Helm, Y. Motorin, HydraPsiSeq: a method for systematic and quantitative mapping of pseudouridines in RNA, Nucleic Acids Res 48 (2020) e110, https://doi.org/10.1093/nar/gkaa769.
[33] L. Ayadi, Y. Motorin, V. Marchand, Quantification of 2'-O-Me residues in RNA using next-generation sequencing (illumina RiboMethSeq protocol), Methods Mol. Biol. 1649 (2018) 29–48, https://doi.org/10.1007/978-1-4939-7213-5_2.
[34] F. Pichot, V. Marchand, L. Ayadi, V. Bourguignon-Igel, M. Helm, Y. Motorin, Holistic optimization of bioinformatic analysis pipeline for detection and quantification of 2′-O-methylations in RNA by RiboMethSeq, Front. Genet. 11 (2020) 38, https://doi.org/10.3389/FGENE.2020.00038/FULL.
[35] V. Marchand, V. Bourguignon-Igel, M. Helm, Y. Motorin, Analysis of pseudouridines and other RNA modifications using HydraPsiSeq protocol, Methods 203 (2022) 383–391, https://doi.org/10.1016/J.YMETH.2021.08.008.
[36] F. Pichot, V. Marchand, M. Helm, Y. Motorin, Data analysis pipeline for detection and quantification of pseudouridine (ψ) in RNA by HydraPsiSeq, Methods Mol. Biol. 2624 (2023) 207–223, https://doi.org/10.1007/978-1-0716-2962-8_14.
[37] T. Efferth, A. Sauerbrey, M.E. Halatsch, D.D. Ross, E. Gebhart, Molecular modes of action of cephalotaxine and homoharringtonine from the coniferous tree Cephalotaxus hainanensis in human tumor cell lines, Naunyn Schmiedebergs Arch. Pharmacol. 367 (2003) 56–67, https://doi.org/10.1007/S00210-002-0632-0.

[38] M. Kulbay, B. Johnson, S. Fiola, R.J. Diaz, J. Bernier, DFF40 deficiency in cancerous T cells is implicated in chemotherapy drug sensitivity and resistance through the regulation of the apoptotic pathway, Biochem. Pharmacol. 194 (2021) 114801, https://doi.org/10.1016/J.BCP.2021.114801.
[39] X. Bo Huang, C. Mei Yang, Q. Mei Han, X. Jin Ye, W. Lei, W. Bin Qian, MNK1 inhibitor CGP57380 overcomes mTOR inhibitor-induced activation of eIF4E: the mechanism of synergic killing of human T-ALL cells, Acta Pharmacol. Sin. 39 (2018) 1894–1901, https://doi.org/10.1038/S41401-018-0161-0; KWRD=BIOMEDICINE.
[40] D. Ivanova, Z. Zhelev, S. Semkova, I. Aoki, R. Bakalova, Resveratrol modulates the redox-status and cytotoxicity of anticancer drugs by sensitizing leukemic lymphocytes and protecting normal lymphocytes, Anticancer Res 39 (2019) 3745–3755, https://doi.org/10.21873/ANTICANRES.13523.
[41] Z. Zhou, X. Lu, J. Wang, J. Xiao, J. Liu, F. Xing, microRNA let-7c is essential for the anisomycin-elicited apoptosis in Jurkat T cells by linking JNK1/2 to AP-1/STAT1/STAT3 signaling, Scientific Reports 2016 6:1 6 (2016) 1–13. https://doi.org/10.1038/srep24434.
[42] C. Rosilio, N. Lounnas, M. Nebout, V. Imbert, T. Hagenbeek, H. Spits, V. Asnafi, R. Pontier-Bres, J. Reverso, J.F. Michiels, I. Ben Sahra, F. Bost, J.F. Peyron, The metabolic perturbators metformin, phenformin and AICAR interfere with the growth and survival of murine PTEN-deficient T cell lymphomas and human T-ALL/T-LL cancer cells, Cancer Lett. 336 (2013) 114–126, https://doi.org/10.1016/J.CANLET.2013.04.015.
[43] E.K. Schmidt, G. Clavarino, M. Ceppi, P. Pierre, SUnSET, a nonradioactive method to monitor protein synthesis, Nat. Methods 6 (2009) 275–277, https://doi.org/10.1038/NMETH.1314.
[44] S. Klinge, J.L. Woolford, Ribosome assembly coming into focus, Nat. Rev. Mol. Cell Biol. 20 (2019) 116–131, https://doi.org/10.1038/S41580-018-0078-Y.
[45] M. Penzo, A. Galbiati, D. Treré, L. Montanaro, The importance of being (slightly) modified: the role of rRNA editing on gene expression control and its connections with cancer, Biochim. Biophys. Acta 2016 (1866) 330–338, https://doi.org/10.1016/J.BBCAN.2016.10.007.
[46] R. Di Francia, S. Crisci, A. De Monaco, C. Cafiero, A. Re, G. Iaccarino, R. De Filippi, F. Frigeri, G. Corazzelli, A. Micera, A. Pinto, Response and toxicity to cytarabine therapy in leukemia and lymphoma: from dose puzzle to pharmacogenomic biomarkers, Cancers (Basel) 13 (2021) 1–39, https://doi.org/10.3390/CANCERS13050966.
[47] E.F. Mason, J.C. Rathmell, Cell metabolism: an essential link between cell growth and apoptosis, Biochim. Biophys. Acta, Mol. Cell Res. 2011 (1813) 645–654, https://doi.org/10.1016/j.bbamcr.2010.08.011.
[48] V.P. Mauro, G.M. Edelman, The ribosome filter hypothesis, Proc. Natl. Acad. Sci. U. S. A. 99 (2002) 12031–12036, https://doi.org/10.1073/PNAS.192442499.
[49] S. Xue, M. Barna, Specialized ribosomes: a new frontier in gene regulation and organismal biology, Nature Reviews Molecular Cell Biology 2012 13:6 13 (2012) 355–369. https://doi.org/10.1038/nrm3359.
[50] N. Segev, J.E. Gerst, Specialized ribosomes and specific ribosomal protein paralogs control translation of mitochondrial proteins, J. Cell Biol. 217 (2018) 117–126, https://doi.org/10.1083/JCB.201706059.
[51] Z. Shi, K. Fujii, K.M. Kovary, N.R. Genuth, H.L. Röst, M.N. Teruel, M. Barna, Heterogeneous ribosomes preferentially translate distinct subpools of mRNAs genome-wide, Mol. Cell 67 (2017) 71–83, https://doi.org/10.1016/J.MOLCEL.2017.05.021.
[52] M.R. Brunchault, A.M. Hesse, J. Schaeffer, A. Fröhlich, A. Saintpierre, C. Decourt, F. Combes, H. Nawabi, Y. Couté, S. Belin, Proteomics-based characterization of ribosome heterogeneity in adult mouse organs, Cell. Mol. Life Sci. 82 (2025), https://doi.org/10.1007/S00018-025-05708-7.
[53] K.R. Kampen, S.O. Sulima, B. Verbelen, T. Girardi, S. Vereecke, G. Rinaldi, J. Verbeeck, J. Op de Beeck, A. Uyttebroeck, J.P.P. Meijerink, A.V. Moorman, C. J. Harrison, P. Spincemaille, J. Cools, D. Cassiman, S.M. Fendt, P. Vermeersch, K. De Keersmaecker, The ribosomal RPL10 R98S mutation drives IRES-dependent BCL-2 translation in T-ALL, Leukemia 33 (2019) 319–332, https://doi.org/10.1038/S41375-018-0176-Z.
[54] K.R. Kampen, L. Fancello, T. Girardi, G. Rinaldi, M. Planque, S.O. Sulima, F. Loayza-Puch, B. Verbelen, S. Vereecke, J. Verbeeck, J. Op de Beeck, J. Royaert, P. Vermeersch, D. Cassiman, J. Cools, R. Agami, M. Fiers, S.M. Fendt, K. De Keersmaecker, Translatome analysis reveals altered serine and glycine metabolism in T-cell acute lymphoblastic leukemia cells, Nat. Commun. 10 (2019), https://doi.org/10.1038/S41467-019-10508-2.
[55] L. Bacci, V. Indio, G. Rambaldelli, C. Bugarin, F. Magliocchetti, A. Del Rio, D. Pollutri, F. Melchionda, A. Pession, M. Lanciotti, C. Dufour, G. Gaipa, L. Montanaro, M. Penzo, Mutational analysis of ribosomal proteins in a cohort of pediatric patients with T-cell acute lymphoblastic leukemia reveals Q123R, a novel mutation in RPL10, Front. Genet. 13 (2022), https://doi.org/10.3389/FGENE.2022.1058468.
[56] S.W. Brady, K.G. Roberts, Z. Gu, L. Shi, S. Pounds, D. Pei, C. Cheng, Y. Dai, M. Devidas, C. Qu, A.N. Hill, D. Payne-Turner, X. Ma, I. Iacobucci, P. Baviskar, L. Wei, S. Arunachalam, K. Hagiwara, Y. Liu, D.A. Flasch, Y. Liu, M. Parker, X. Chen, A.H. Elsayed, O. Pathak, Y. Li, Y. Fan, J.R. Michael, M. Rusch, M. R. Wilkinson, S. Foy, D.J. Hedges, S. Newman, X. Zhou, J. Wang, C. Reilly, E. Sioson, S.V. Rice, V. Pastor Loyola, G. Wu, E. Rampersaud, S.C. Reshmi, J. Gastier-Foster, J.M. Guidry Auvil, P. Gesuwan, M.A. Smith, N. Winick, A. J. Carroll, N.A. Heerema, R.C. Harvey, C.L. Willman, E. Larsen, E.A. Raetz, M. J. Borowitz, B.L. Wood, W.L. Carroll, P.A. Zweidler-McKay, K.R. Rabin, L. A. Mattano, K.W. Maloney, S.S. Winter, M.J. Burke, W. Salzer, K.P. Dunsmore, A. L. Angiolillo, K.R. Crews, J.R. Downing, S. Jeha, C.H. Pui, W.E. Evans, J.J. Yang, M. V. Relling, D.S. Gerhard, M.L. Loh, S.P. Hunger, J. Zhang, C.G. Mullighan, The genomic landscape of pediatric acute lymphoblastic leukemia, Nat. Genet. 54 (2022) 1376–1389, https://doi.org/10.1038/s41588-022-01159-z.
[57] J.A. Doudna, V.L. Rath, Structure and function of the eukaryotic ribosome: the next frontier, Cell 109 (2002) 153–156, https://doi.org/10.1016/S0092-8674(02)00725-0.
[58] S. Robledo, R.A. Idol, D.L. Crimmins, J.H. Ladenson, P.J. Mason, M. Bessler, The role of human ribosomal proteins in the maturation of rRNA and ribosome production, RNA 14 (2008) 1918–1929, https://doi.org/10.1261/RNA.1132008.
[59] J. Bertram, K. Palfner, W. Hiddemann, M. Kneba, Overexpression of ribosomal proteins L4 and L5 and the putative alternative elongation factor PTI-1 in the doxorubicin resistant human colon cancer cell line LoVoDx(R), Eur. J. Cancer 34 (1998) 731–736, https://doi.org/10.1016/S0959-8049(97)10081-8.
[60] J. Aspden, W.J. Faller, M. Barna, A. Lund, Ribosome heterogeneity and specialization, Philos. Trans. R. Soc. Lond. B Biol. Sci. 380 (2025), https://doi.org/10.1098/RSTB.2023.0375.
[61] A.L. Wolfe, K. Singh, Y. Zhong, P. Drewe, V.K. Rajasekhar, V.R. Sanghvi, K. J. Mavrakis, M. Jiang, J.E. Roderick, J. Van der Meulen, J.H. Schatz, C.M. Rodrigo, C. Zhao, P. Rondou, E. de Stanchina, J. Teruya-Feldstein, M.A. Kelliher, F. Speleman, J.A. Porco, J. Pelletier, G. Rätsch, H.G. Wendel, RNA G-quadruplexes cause eIF4A-dependent oncogene translation in cancer, Nature 513 (2014) 65–70, https://doi.org/10.1038/NATURE13485.
[62] A. Schwarzer, H. Holtmann, M. Brugman, J. Meyer, C. Schauerte, J. Zuber, D. Steinemann, B. Schlegelberger, Z. Li, C. Baum, Hyperactivation of mTORC1 and mTORC2 by multiple oncogenic events causes addiction to eIF4E-dependent mRNA translation in T-cell leukemia, Oncogene 34 (2015) 3593–3604, https://doi.org/10.1038/ONC.2014.290.
[63] B.P. De Conti, A. Miluzio, F. Grassi, S. Abrignani, S. Biffo, S. Ricciardi, MTOR-dependent translation drives tumor infiltrating cd8+ effector and cd4+ Treg cells expansion, Elife 10 (2021), https://doi.org/10.7554/ELIFE.69015.
[64] M. Liu, F. Liu, Resveratrol inhibits mTOR signaling by targeting DEPTOR, Commun. Integr. Biol. 4 (2011) 382–384, https://doi.org/10.4161/CIB.15309.
[65] I. Ben Sahra, C. Regazzetti, G. Robert, K. Laurent, Y. Le Marchand-Brustel, P. Auberger, J.F. Tanti, S. Giorgetti-Peraldi, F. Bost, Metformin, independent of AMPK, induces mTOR inhibition and cell-cycle arrest through REDD1, Cancer Res. 71 (2011) 4366–4372, https://doi.org/10.1158/0008-5472.CAN-10-1769.
[66] A.M. Poodeh, G.A. Sarab, M.P. Ravari, M. Najafzadeh, H. Safarpour, A. Zarban, M. Sayadi, S.M. Sajjadi, Metformin and chloroquine enhanced the efficacy of cytarabine in acute lymphoblastic leukemia cell lines: a drug repositioning approach, Sci. Rep. 15 (2025) 1–16, https://doi.org/10.1038/s41598-025-01574-2.
[67] M. Trucco, J.C. Barredo, J. Goldberg, G.M. Leclerc, G.A. Hale, J. Gill, B. Setty, T. Smith, R. Lush, J.K. Lee, D.R. Reed, A phase I window, dose escalating and safety trial of metformin in combination with induction chemotherapy in relapsed refractory acute lymphoblastic leukemia: Metformin with induction chemotherapy of vincristine, dexamethasone, PEG-asparaginase, and doxorubicin, Pediatr. Blood Cancer 65 (2018), https://doi.org/10.1002/PBC.27224.
[68] P. Quist-Paulsen, N. Toft, M. Heyman, J. Abrahamsson, L. Grišk evičius, H. Hallböök, G. Jónsson, K. Palk, G. Vaitkeviciene, K. Vettenranta, A. Åsberg, T. L. Frandsen, S. Opdahl, H.V. Marquart, S. Siitonen, L.T. Osnes, M. Hultdin, U. M. Overgaard, U. Wartiovaara-Kautto, K. Schmiegelow, T-cell acute lymphoblastic leukemia in patients 1–45 years treated with the pediatric NOPHO ALL2008 protocol, Leukemia 34 (2020) 347–357, https://doi.org/10.1038/s41375-019-0598-2.
[69] E. De Schutter, B. Cappe, B. Wiernicki, P. Vandenabeele, F.B. Riquet, Plasma membrane permeabilization following cell death: many ways to dye!, Cell Death Discov. 7 (2021) 1–3, https://doi.org/10.1038/S41420-021-00545-6.
[70] N.D. Vincelette, S. Yun, Assessing the mechanism of cytarabine-induced killing in acute leukemia, Blood 124 (2014) 5210, https://doi.org/10.1182/BLOOD.V124.21.5210.5210.
[71] Y. Liu, J. Ge, Q. Li, L. Gu, X. Guo, Z.G. Ma, Y.P. Zhu, Anisomycin induces apoptosis of glucocorticoid resistant acute lymphoblastic leukemia CEM-C1 cells via activation of mitogen-activated protein kinases p38 and JNK, Neoplasma 60 (2013) 101–110, https://doi.org/10.4149/NEO_2013_014.
[72] L. Yinjun, J. Jie, X. Weilai, T. Xiangming, Homoharringtonine mediates myeloid cell apoptosis via upregulation of pro-apoptotic bax and inducing caspase-3-mediated cleavage of poly(ADP-ribose) polymerase (PARP), Am. J. Hematol. 76 (2004) 199–204, https://doi.org/10.1002/AJH.20100.
[73] Q. Wang, X. Wei, Research progress on the use of metformin in leukemia treatment, Curr. Treat. Options Oncol. 25 (2024) 220–236, https://doi.org/10.1007/S11864-024-01179-3.
[74] P. Li, S. Diab, M. Yu, J. Adams, S. Islam, S.K.C. Basnet, H. Albrecht, R. Milne, S. Wang, Inhibition of Mnk enhances apoptotic activity of cytarabine in acute myeloid leukemia cells, Oncotarget 7 (2016) 56811–56825, https://doi.org/10.18632/ONCOTARGET.10796.
[75] A. Pelava, C. Schneider, N.J. Watkins, The importance of ribosome production, and the 5S RNP-MDM2 pathway, in health and disease, Biochem. Soc. Trans. 44 (2016) 1086–1090, https://doi.org/10.1042/BST20160106.
[76] H. Lee, J.H. Jung, H.M. Ko, H. Park, A.M. Segall, R.L. Sheffmaker, J. Wang, W. D. Frey, N. Pham, Y. Wang, Y. Zhang, J.G. Jackson, S.X. Zeng, H. Lu, RNA-binding motif protein 10 inactivates c-Myc by partnering with ribosomal proteins uL18 and uL5, Proc. Natl. Acad. Sci. U. S. A. 120 (2023), https://doi.org/10.1073/PNAS.2308292120.